

Chemically Robust Indium Tin Oxide/Graphene Anode for Efficient Perovskite Light-Emitting Diodes

Sung-Joo Kwon,[▽] Soyeong Ahn,[▽] Jung-Min Heo,[▽] Dong Jin Kim, Jinwoo Park, Hae-Ryung Lee, Sungjin Kim, Huanyu Zhou, Min-Ho Park, Young-Hoon Kim, Wanhee Lee, Jeong-Yun Sun, Byung Hee Hong, and Tae-Woo Lee*



Cite This: <https://dx.doi.org/10.1021/acsami.0c12939>



Read Online

ACCESS |



Metrics & More



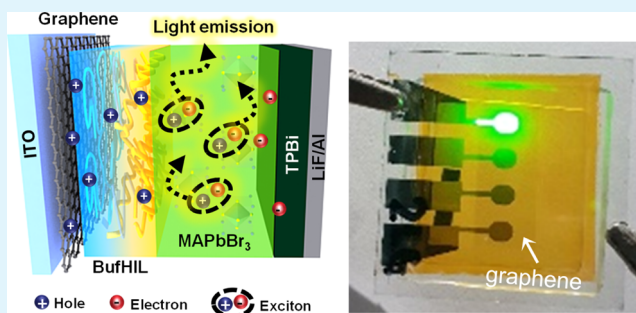
Article Recommendations



Supporting Information

ABSTRACT: Graphene is an optimal material to be employed as an ionic diffusion barrier because of its outstanding impermeability and chemical robustness. Indium tin oxide (ITO) is often used in perovskite light-emitting diodes (PeLEDs), and it can release indium easily upon exposure to the acidic hole-injection layer so that luminescence can be quenched significantly. Here, we exploit the outstanding impermeability of graphene and use it as a chemical barrier to block the etching that can occur in ITO exposed to an acidic hole-injection layer in PeLEDs. This barrier reduced the luminescence quenching that these metallic species can cause, so the photoluminescence lifetime of perovskite film was substantially higher in devices with ITO and graphene layer (87.9 ns) than in devices that had only an ITO anode (22.1 ns). Luminous current efficiency was also higher in PeLEDs with a graphene barrier (16.4 cd/A) than in those without graphene (9.02 cd/A). Our work demonstrates that graphene can be used as a barrier to reduce the degradation of transparent electrodes by chemical etching in optoelectronic devices.

KEYWORDS: graphene, barrier, perovskite, exciton quenching, light-emitting diodes



1. INTRODUCTION

Perovskite light-emitting diodes (PeLEDs) have advantages of low fabrication cost and high color purity.^{1–3} Various chemical modifications [e.g., stoichiometry control, nanocrystal pinning (NCP), and additive engineering] of perovskite emitting layers to overcome the luminescence quenching have achieved significant increases in the luminous properties of PeLEDs.^{2,3} However, their luminous properties are severely degraded by luminescence quenching that is caused by low exciton binding energy (BE) in polycrystalline perovskites.

Indium tin oxide (ITO) is the most widely used transparent electrode in modern electronic devices. It is often combined with a hole-injection layer (HIL) composed of poly(3,4-ethylenedioxythiophene) polystyrene sulfonate (PEDOT:PSS) which is very acidic (pH ~2). ITO is vulnerable to acids, so it releases metallic species, especially Indium (In), when it is etched by PEDOT:PSS. These metallic species diffuse into overlying layers, and they cause severe luminescence quenching at the interface between PEDOT:PSS and the perovskite emitting layer.^{4,5} A barricade to this diffusion of metal species from ITO can reduce luminescence quenching and yield efficient PeLEDs. Reduction of quenching of luminescence in PeLEDs has been achieved in several ways, including: (i) choosing a polymeric HIL that is less acidic than PEDOT:PSS;⁶ (ii) blending a fluorinated ionomer with PEDOT:PSS;^{3–5} and

(iii) replacing ITO with other transparent conducting electrodes (TCEs) (e.g., graphene,⁵ conducting polymers^{2,7}). However, the ITO anode/PEDOT:PSS HIL system is still the most widely used in the research. Ideally, the structure of the anode in this system should be modified to eliminate the leaching problem.

Here, we demonstrate that graphene on ITO can effectively block the diffusion of metallic species from ITO to the perovskite layer. This blockage is possible because of graphene's chemical robustness and good ability to impede the penetration of gaseous or ionic species.^{8–11} Because of this property with massive productivity,⁹ graphene has been evaluated as an encapsulation layer in organic electronics.^{12–14} Applying graphene on transparent electrodes (transparent electrodes, metallic nanowires), we confirmed that graphene can be used as a barrier on transparent electrodes that suffer from instability in acidic conditions. We inserted a graphene layer between an ITO anode and a PEDOT:PSS HIL to block the release of In and Sn

Received: July 19, 2020

Accepted: December 11, 2020

from ITO in response to PEDOT:PSS etching. Graphene barrier prevents diffusion of metallic species from the anode to the perovskite layer and thereby increases the luminous efficiency of PeLEDs by preventing the luminescence quenching that diffused In species cause at the interface between perovskite- and PEDOT:PSS-based HILs.

2. EXPERIMENTAL SECTION

Single-layer graphene (SLG) was synthesized on Cu foil by chemical-vapor deposition (CVD). Cu foils were heated to ~ 1000 °C with 15 sccm flow of H_2 for 30 min and 60 sccm of CH_4 gas as a carbon feedstock and then cooled down to room temperature. Then, polymethylmethacrylate (PMMA) solution (dissolved in chlorobenzene) was spin-coated to support graphene during the wet-transfer process. Synthesized graphene on back-side of Cu foil was removed by O_2 plasma treatment using reactive ion etching (RIE). SLG-grown Cu foil was floated in ammonium persulfate solution to etch away the Cu, and then rinsed with deionized (DI) water several times to remove the residual etchant. The floating SLG/PMMA was transferred onto target substrates. The PMMA layer was removed by soaking the graphene-transferred substrate several times in an acetone bath. To obtain two-layer graphene (2LG) and three-layer graphene (3LG), this stacking process was repeated.

To measure the ion transport, we built an apparatus that is composed of two sinks that are separated except for a layer of graphene that has been transferred onto a dialysis membrane (molecular cutoff: 1,000) (Figure S1, Supporting Information). DI water and 0.1 M HCl solution were injected into two sinks at the same speed, and ion conductivity in the DI water sink was measured using Ag/AgCl electrodes and an electrochemical analyzer (MP3, ZIVE).

To prepare methylammonium lead bromide ($CH_3NH_3PbBr_3$, MAPbBr₃) film, methylammonium bromide (CH_3NH_3Br , Dyesol) and lead bromide ($PbBr_2$, Sigma-Aldrich) were mixed at 1.06:1 (molar ratio) and dissolved in dimethylsulfoxide (Sigma-Aldrich) at room temperature for >3 h.

MAPbBr₃ films were fabricated by spin-coating the precursor solution in two steps (500 rpm for 5 s; 3000 rpm for 60 s, successively) under a N_2 atmosphere. Additive-assisted NCP was used to achieve a high-quality perovskite film with nanometer grain size:² during the second spin step, chloroform with 2,2',2''-(1,3,5-benzinetriyl)-tris(1-phenyl-1-*H*-benzimidazole) (TPBi) was dropped onto the spinning perovskite film. The prepared MAPbBr₃ films were baked on a hotplate at 90 °C for 10 min.

ITO-patterned glass substrates were cleaned by ultrasonic treatment in acetone for 15 min and then in isopropyl alcohol for 15 min. Graphene on ITO was patterned by O_2 plasma treatment using an RIE system. The resulting ITO/graphene surface was made hydrophilic by ultraviolet–ozone (UVO) treatment. We used a previously described method⁵ to synthesize a HIL (BufHIL) that has a gradient work function by inducing self-organization of PEDOT:PSS (CLEVIOS P VP AI4083) and tetrafluoroethylene-perfluoro3,6-dioxo-4-methyl-7-octene-sulfonic acid copolymer (PFI); the solution was spin-coated to form 100 nm thickness and then annealed at 150 °C for 30 min. After the MAPbBr₃ film had been formed on the BufHIL-coated substrate, TPBi (50 nm), LiF (1 nm), and Al (100 nm) were sequentially deposited in a thermal evaporator under high vacuum ($<10^{-7}$ Torr). The fabricated PeLEDs were encapsulated under a N_2 atmosphere by using a glass lid and UV-curable epoxy resin.

Images of the surfaces were obtained using a field-emission scanning electron microscope (SUPRA 55VP). Surface topography was measured using an atomic force microscope (NX-10, Park Systems). X-ray photoelectron spectroscopy (XPS) measurements of BufHIL on ITO and on ITO/graphene were conducted in collaboration with the Korea Basic Science Institute (KBSI). Time-of-flight secondary ion mass spectrometry (TOF-SIMS) was performed at the KBSI with a 30 keV Bi^+ beam. Steady-state photoluminescence (PL) and PL lifetime were measured using a fluorescence spectrometer (FluoroTime 300); the MAPbBr₃ film was excited using a 405 nm-wavelength laser equipped with a picosecond-pulse laser head (LD H-P-C-405B,

PicoQuant). To measure PL lifetime, a photon-counting detector (PMA Hybrid 07) and time-correlated single-photon counting (TCSPC) module (PicoHarp, PicoQuant) were used. The transmission electron microscopy (TEM) analysis was performed using a Tecnai F20 operating at an acceleration voltage of 200 kV. The TEM samples were prepared by using the focused ion beam (FIB, SMI3050SE) system with a 30 kV gallium liquid metal ion source.

3. RESULTS AND DISCUSSION

We used graphene as an etching barrier on ITO to prevent migration of metallic species and the luminescence quenching that they cause during PeLED operation (Figure 1). When

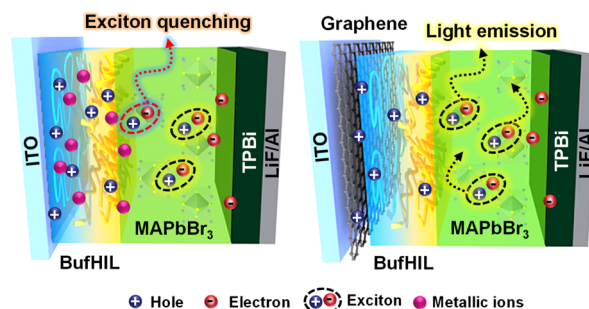


Figure 1. Schematics of exciton quenching by diffused metallic ions (left) and efficient light emission by insertion of graphene (right) in PeLEDs.

transferred using conventional wet-transfer methods,¹⁵ CVD-grown SLG has several defects including pores, wrinkles, and scrolls (Figure 2a).^{12,16} SLG has pores of various sizes ranging from several tens of nanometers to sub-micrometers (Figure 2a,b). However, when two SLG layers are stacked, they patch each other by covering these pores (Figure 2c,d). To ensure the scalability of graphene patching effect, we observed randomly selected four spots of a graphene sample and measured randomly selected two R_s maps of large areas (> 2 cm \times 2 cm). The patching effect is confirmed in every spot of graphene (Figure S1a–d), and each R_s map exhibited outstanding uniformity (Figure S1e); it demonstrates the patching effect of graphene stacking with large-area uniformity. Even single-layered graphene has pores which are large enough for metallic species to go through; however, the area that allows penetration is reduced (Figure S1f,g). As the number of graphene layers increased, the thickness of graphene increased (Figure S1h); thus, metal atomic species that penetrate the first graphene barrier face another graphene barrier and thus the penetration path length of the metal atomic species increased. This patching would increase the sieving capacity of graphene.

We directly monitored the improved sieving capacity of stacked graphene by using a home-made ion-transport apparatus (Figure S2a). To support the ultrathin SLG, we used a dialysis membrane (molecular cutoff: 1000) as a substrate (Figure S2b). The dialysis membrane is ion-permeable, so the initial ionic current between the two electrodes was >3 μA after ~ 1 min and showed continuous increase. However, 1LG on the membrane reduced the ionic current by $>80\%$ after 6 min, and stacking 2LG and 3LG reduced the current further. These results demonstrated that graphene stacking can effectively reduce the transport of H^+ ions; so, graphene is plausible as a barrier to protect ITO from PEDOT:PSS.¹⁷

To confirm the applicability of graphene as a barrier on ITO, we dipped ITO and ITO/graphene into an acidic solution (1.0

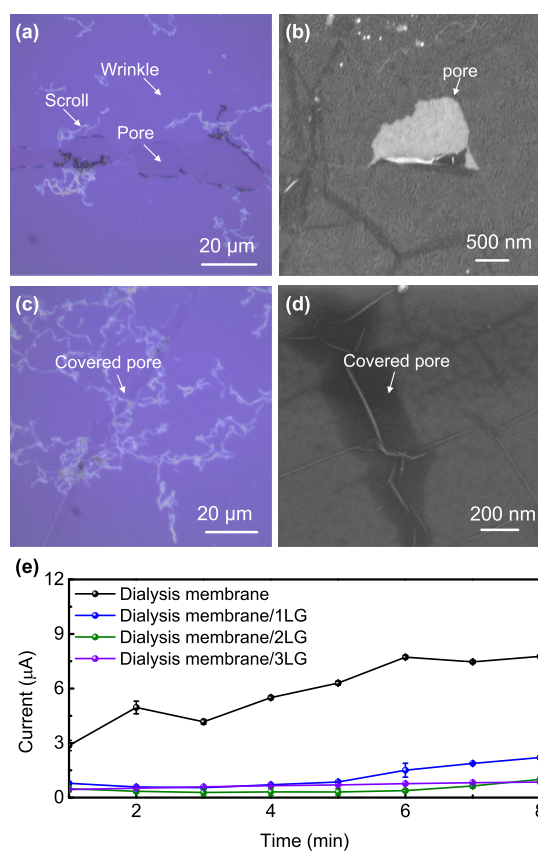


Figure 2. Improved barrier properties to ion transport by graphene stacking. Optical microscopy image and SEM image of (a,b) single-layered graphene and (c,d) multilayer stacked graphene. (e) Diffusive transport rate of 0.1 M HCl solution through graphene on dialysis membrane. Inset: photographs of transferred graphene on dialysis membrane.

M HCl) and monitored the etching behavior (Figure 3a–c). In atomic force microscopy topographic images, the height difference between substrate and transferred graphene was only ~ 2 nm (Figure S3), whereas the height difference of the boundary between ITO and ITO/graphene was ~ 12 nm (Figure 3b), that is, ~ 10 nm of this height difference can be attributed to the reduced etching ITO beneath the graphene. This difference clearly shows that graphene prevents the etching of ITO in an acidic solution. This observation coincides with transmittance changes of ITO and of ITO/graphene in acidic conditions. The transmittance changed less in the ITO/graphene anode than in the ITO-only anode; this difference can also be attributed to the capacity of graphene to prevent the etching of ITO. The use of 2LG and 3LG increased this protection effect of graphene on ITO (Figure 3c). We additionally tested the prevention effect of graphene on ITO against various acidic solutions (i.e., CH_3COOH , HNO_3) (Figure S4a,b). Similar to the dipping test in HCl, transmittance changes of ITO/graphene in other acid solutions were smaller than those of ITO; it proves that the graphene barrier is a versatile barrier platform in various acidic conditions.

To quantify the feasibility of graphene as a barrier to protect another type of TCEs, we considered silver nanowires (AgNWs), which are also vulnerable to acidity.¹⁸ We compared corrosion in bare AgNWs to that in AgNWs that had been covered with graphene (AgNWs/graphene) (Figure 3d). The AgNWs were dipped into a 1.0 M HCl solution; after 1 h, bare

AgNWs were severely oxidized and showed serious disconnection and oxidation (Figure 3d),¹⁸ whereas AgNWs/graphene were virtually undamaged (Figure 3d). In bare AgNWs, the sheet resistance R_s increased greatly, but in AgNWs/graphene, this change was small and decreased as the number of graphene layers increased (Figure 3e). These results indicate that graphene may be an excellent barrier platform for various TCEs under various chemical circumstances.

To quantify the diffusion behavior of In species in the perovskite layer, we performed TOF-SIMS on films composed of perfluorinated ionomer-blended PEDOT:PSS (BufHIL) abutted to perovskite (MAPbBr_3) on ITO or on ITO/graphene (Figure 4a,b). Both Pb^+ and CF^+ ions formed in the ITO and ITO/graphene-based samples; Pb^+ comes from the top MAPbBr_3 layer, and CF^+ comes from the BufHIL. The spectral peak of CF^+ started to increase at ~ 400 s of sputter time; this result implies that the interface between MAPbBr_3 and BufHIL begins to form after ~ 400 s of sputtering. The spectral peak of In^+ began to increase after that of CF^+ in both ITO-only and ITO/graphene-based samples; this change shows that In^+ exists in the polymeric HILs but not in the MAPbBr_3 bulk layer. Notably, In^+ peak increased later in the spectrum of ITO/graphene than in that of ITO only (Figure 4a,b), and stacking of graphene on ITO induces additional delay in the increase of the In^+ peak (toward the bottom surface) (Figure S5). We also performed XPS on polymeric HILs on ITO/graphene and ITO only (Figure 4c,d). Clear In 3d peaks were observed in XPS spectra from polymeric HILs on ITO or ITO/1LG. To deposit polymeric HILs on a hydrophobic graphene layer, UVO treatment was performed; this procedure etches the graphene surface, and this may be the reason that the diffusion-blocking effect is weak in ITO/1LG.¹⁹ As the number of stacked graphene layers increased, the In 3d peaks decreased, and ITO/3LG showed similar spectra to HILs on glass that has no In species; this result indicates that 3LG almost perfectly blocks In diffusion into the top region of polymeric HILs (Figure 4c,d). Both TOF-SIMS and XPS results prove that graphene effectively blocks metal diffusion between layers in PeLEDs.

To verify that this reduced diffusion of metallic species improved the luminous properties of MAPbBr_3 , steady-state PL and time-resolved PL were quantified (Figure 5a,b). As graphene layers stacked on ITO, the intensity of steady-state PL increased (Figure 5a). To investigate the exciton kinetics and to determine how the blocked metal diffusion affects luminous properties, TCSPC was conducted. PL intensity decayed rapidly in MAPbBr_3 on ITO/BufHIL but slowly on ITO/2LG/BufHIL (Figure 5b). Both PL decay curves were fitted using a bi-exponential decay model.^{2,5,6} A fit to the decay model indicated that MAPbBr_3 on ITO/BufHIL had PL lifetime $\tau \sim 22.1$ ns, which matches well with the previous results.⁵ After graphene insertion, PL lifetime was increased by a factor of ~ 4 ($\tau \sim 87.9$ ns).

MAPbBr_3 on both ITO and ITO/graphene exhibit the same XRD patterns and similar surface morphology (Figure S6 and S7); this similarity indicates that crystalline structures of MAPbBr_3 were similar to those on ITO and ITO/graphene; that is, diffused In from etched ITO do not change the morphology of overlying MAPbBr_3 films. Therefore, the increased PL intensity and PL lifetime can be attributed solely to the prevented diffusion of In.

To prove that reduced quenching influenced the increased properties, we also measured the PL lifetime of colloidal formamidinium $[\text{FA}, \text{CH}(\text{NH}_2)_2]$ lead bromide perovskite

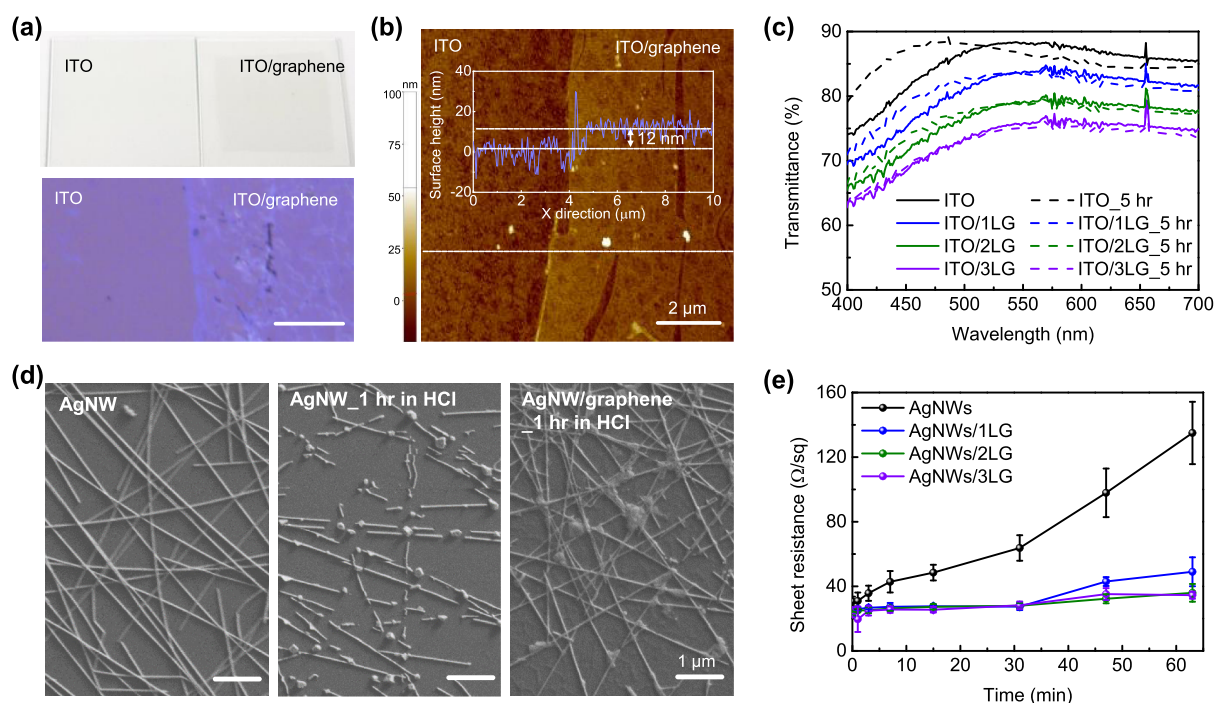


Figure 3. Stability of pristine transparent conducting oxides and transparent conducting materials with graphene. (a) Photograph of ITO and ITO/graphene (top) and optical microscopy image of boundary region of graphene transferred on ITO (bottom). Scale bar = 30 μm . (b) Atomic force microscopy image of boundary region of graphene transferred on etched ITO by dipping into the 1.0 M HCl solution for 5 h. Inset: surface height along the white dashed line. Scale bar = 2 μm . (c) Transmittance change of ITO and ITO/graphene after dipping into HCl solution. (d) SEM image of the as-prepared AgNWs (left), AgNWs after 1 h in the 1.0 M HCl solution (middle), and AgNWs/graphene after 1 h in the 1.0 M HCl solution (right). Scale bar = 1 μm . (e) Sheet resistance change of AgNWs and AgNW/graphene after dipping in HCl solution.

nanoparticles (FAPbBr₃ NPs). FAPbBr₃ NPs have a much smaller grain size (~ 10 nm) than MAPbBr₃ polycrystalline film (0.1–10 μm), FAPbBr₃ NPs are covered by insulating ligands,^{3,20} and FAPbBr₃ NPs can have higher exciton BE than the polycrystalline counterpart and thus have less effect on exciton quenching than the MAPbBr₃ polycrystalline films do.

The time-resolved PL results of FAPbBr₃ NPs do not show noticeable changes as the number of stacked graphene layer changes (Figure S8); this result is in contrast to those of MAPbBr₃ polycrystalline films, which exhibit a notable increase of PL lifetime as this number increases. The result also indicates that graphene on ITO can effectively extend the PL lifetime of perovskite polycrystalline films that have low exciton BE.

PeLEDs with BuFHILs were fabricated on ITO anodes and ITO/graphene anodes (Figure 5c–f). Our BuFHIL has high surface potential (~ 5.95 eV),⁴ which facilitates hole injection from an anode to an overlying MAPbBr₃ layer (Figure S9). TEM images clearly show the lattice structure of graphene between ITO and BuFHIL, indicating that the graphene layer is stably maintained during the fabrication of PeLEDs with ITO/graphene anodes (Figure S10). At first, we tested the luminous properties of PeLEDs that have ITO, ITO/1LG, ITO/2LG, and ITO/3LG (Figure S11). PeLEDs with graphene-stacked ITO exhibited higher luminance at the same current density, indicating that the stacked graphene on ITO reduces the luminance quenching in PeLEDs. As the number of stacked graphene (n) increases, luminance characteristics showed saturation behavior at $n = 2$ (Figure S11). However, PeLEDs with $n = 3$, exhibit similar luminance at < 60 mA/cm² of current density or lower region, which can be attributed to a trade-off between the reduced optical transparency of ITO/graphene anode and reduced luminescence quenching. Employing

conventional wet-transfer methods, graphene inevitably has transfer residues and they accumulate as n increases. Transfer residues (e.g., PMMA, Cu etchant, H₂O) protrude from graphene and thus induce the electrical leakage current, causing instable operation in thin-film optoelectronics. Thus, increasing n in PeLEDs reduces luminous quenching, increases electrical leakage current, and decreases the transmittance by graphene. In our work, we employed $n = 2$ as an optimized n in PeLEDs to show the barrier characteristics of graphene. We additionally tested graphene as an etching barrier for the AgNW electrode. In contrast to the ITO-based system, PeLEDs with AgNW/graphene did not show luminescence (Figure S12a). During the PeLED fabrication, UVO treatment is required on AgNWs/graphene to make a hydrophilic surface to form a BuFHIL layer on AgNWs/graphene. However, UVO treatment severely increases the R_s of AgNW, and hole injection from AgNWs to an overlying layer in PeLEDs is substantially disturbed (Figure S12b). The 2LG was doped with HNO₃ by vapor treatment to improve the electrical conductivity of the resulting ITO/2LG anode in PeLEDs.^{21,22} HNO₃ reduced the R_s by $\sim 51\%$ ($R_{s,\text{pristine}} = 255.3$ Ω/sq , $R_{s,\text{doped}} = 125.4$ Ω/sq). The graphene barrier prevented exciton quenching, so PeLEDs that had ITO/2LG achieved higher maximum current efficiency (CE) and external quantum efficiency (EQE) than those of ITO ($\text{CE}_{\text{ITO}} = 9.02$ cd/A, $\text{EQE}_{\text{ITO}} = 2.07\%$, $\text{CE}_{\text{ITO/2LG}} = 16.4$ cd/A, $\text{EQE}_{\text{ITO/2LG}} = 3.76\%$) (Figure 5c,f). All of the PeLEDs exhibited green electroluminescence (centered at 542 nm) with high color purity (full width half maximum < 20 nm) (Figure 5f). To ensure the repeatability of the ITO/2LG anode in PeLEDs, we fabricated six PeLEDs with three ITO anodes and three ITO/2LG anodes (Figure S13). CEs and EQEs of PeLEDs using ITO/2LG anode consistently showed superior luminous

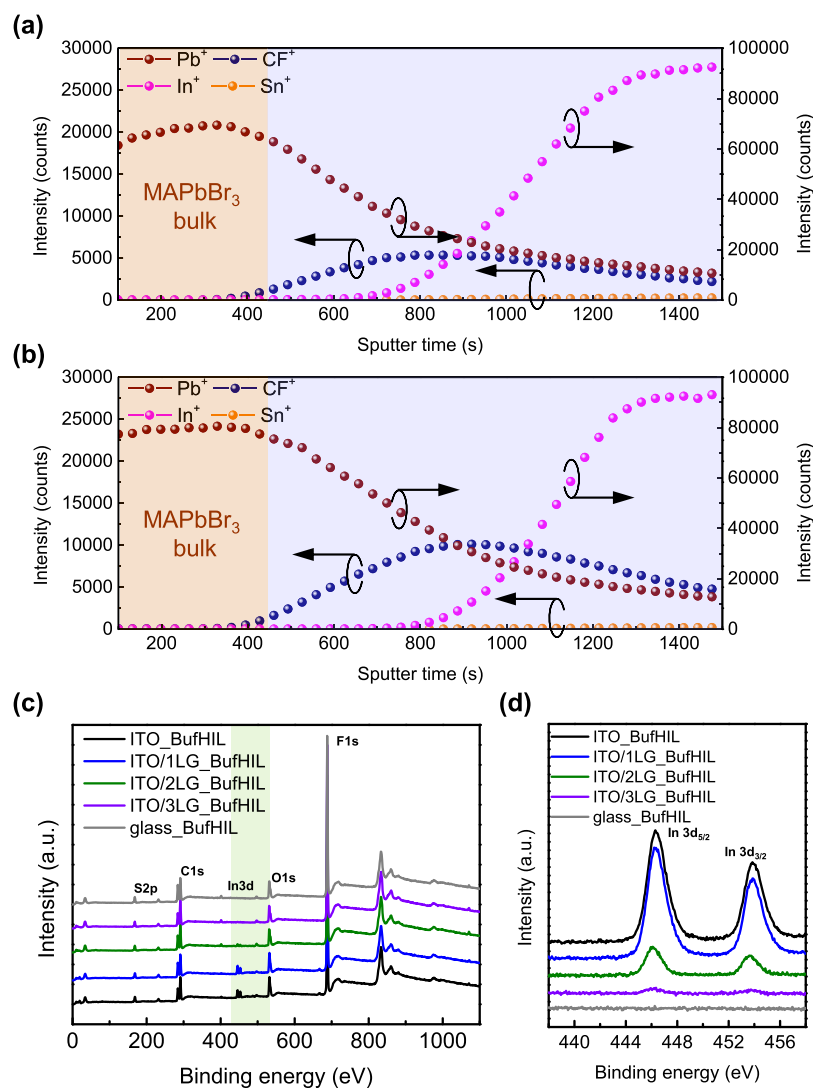


Figure 4. Compositional analysis of metallic ion diffusions on ITO and ITO/graphene into overlying layers. TOF-SIMS results of polymeric HILs and MAPbBr₃ on (a) ITO and (b) ITO/graphene. XPS (c) survey spectra and (d) In 3d spectra of BufHIL on ITO and ITO/graphene.

properties than those of ITO anodes, which can prove the reproducibility of ITO/2LG anodes in PeLEDs.

To quantify how graphene insertion affected the hole-injecting properties of the ITO anode, we fabricated hole-only devices (HODs) and compared the hole current densities (Figure S14).^{21–23} We used ~ 1.8 μm -thick *N,N'*-di(1-naphthyl)-*N,N'*-diphenyl(1,1'-biphenyl)-4,4'-diamine as a hole transport layer on top of various anodes (ITO, ITO/2LG) and BufHILs (Figure S14a). Introducing 2LG changed the anode surface of ITO/2LG, but the decrease in hole-current density in HODs was negligible (Figure S14b). This is because the surface of the anodes was covered by BufHIL which has high surface potential irrespective of the anode. Because PFI locates at the surface of BufHIL due to its low surface energy and PEDOT:PSS locates at the bulk region of BufHIL, both electrodes (i.e., ITO, ITO/2LG) have electrical contact with bulk PEDOT:PSS and they have the same surface potential after BufHIL deposition on the anodes, resulting in similar hole-injecting properties. We conclude that graphene insertion effectively blocks the etching of ITO and thereby increases the luminous efficiency of PeLEDs by preventing the luminescence

quenching of perovskite emitting layers without reducing the hole-injecting capability of the ITO anode.²³

4. CONCLUSIONS

We inserted graphene as a chemical barrier to block the diffusion of metal species between ITO and PEDOT:PSS in PeLEDs. We confirmed that graphene on a dialysis membrane can effectively block ion transport and that as graphene layers are stacked, each bandage the pores in the others, so this blocking ability increases. By using graphene barriers on various transparent electrodes that suffer from chemical vulnerability, we confirmed that graphene reduced their degradation during exposure to acid. Chemical analysis on ITO/graphene/acidic HIL/perovskite layer demonstrated that graphene effectively prevents the etching of ITO and thereby substantially blocks diffusion of In from underlying ITO to an overlying perovskite layer; therefore, PeLEDs that had this barrier achieved substantially higher luminous current efficiency ($CE_{\text{ITO/2LG}} = 16.4$ cd/A) than did PeLEDs that lacked it ($CE_{\text{ITO}} = 9.02$ cd/A). This work can be intended to provide a promising guideline for how graphene can be used as a barrier material in transparent electrodes for optoelectronics.

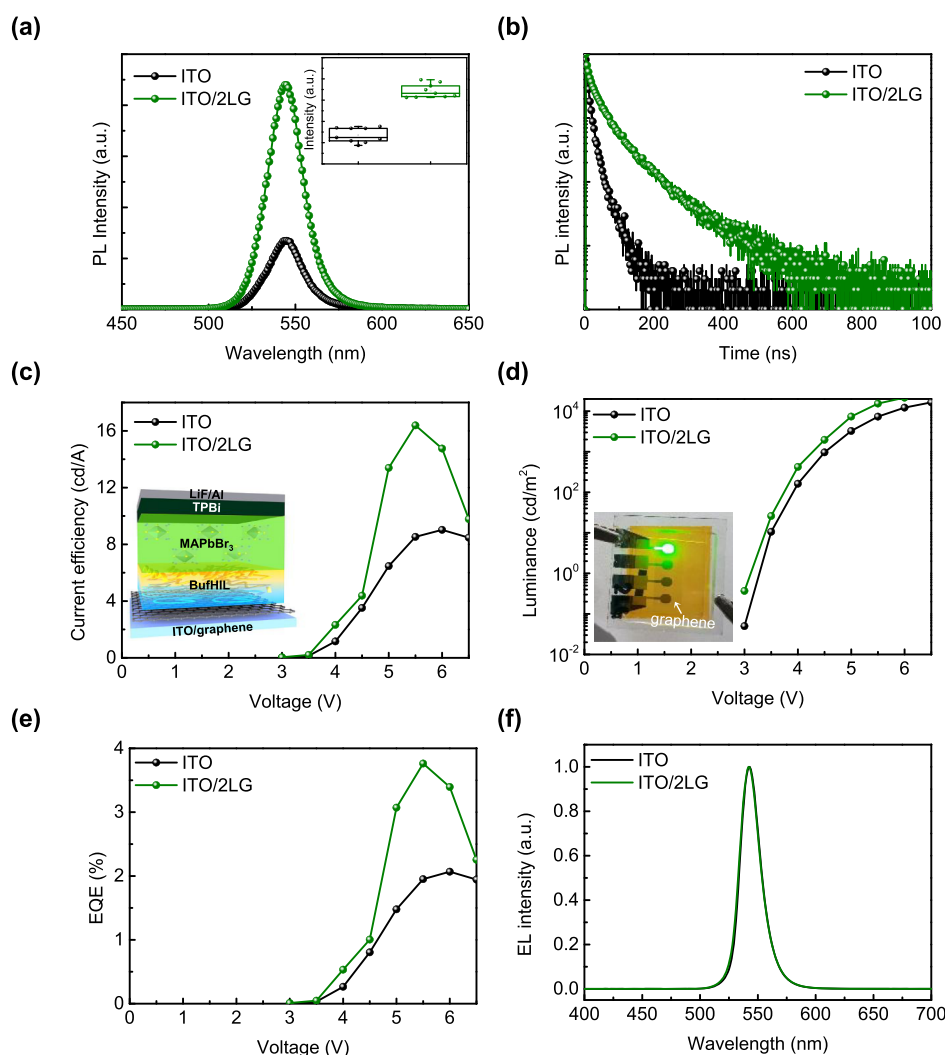


Figure 5. Luminous properties of MAPbBr₃ film and LEDs using MAPbBr₃ emitting layers. (a) Steady-state PL spectra and (b) PL lifetime of BufHIL/MAPbBr₃ film on ITO and ITO/graphene. (c) Current efficiencies, (d) luminance, (e) EQEs, and (f) EL spectra of PeLEDs with ITO and ITO/graphene.

ASSOCIATED CONTENT

Supporting Information

The Supporting Information is available free of charge at <https://pubs.acs.org/doi/10.1021/acsami.0c12939>.

Schematics of ion transport measurement apparatus, atomic force microscopy images of ITO/graphene, changes of TOF-SIMS, X-ray diffraction patterns, scanning electron microscopy images of ITO/graphene/BufHIL/MAPbBr₃ depending on the number of graphene layers on ITO, TCSPC results of MAPbBr₃ and FAPbBr₃ NPs on ITO/graphene/BufHIL, and device characteristics of HODs with the various anodes (ITO, ITO/2LG) (PDF)

AUTHOR INFORMATION

Corresponding Author

Tae-Woo Lee – Department of Materials Science and Engineering, Research Institute of Advanced Materials, Institute of Engineering Research, Nano Systems Institute (NSI), and School of Chemical and Biological Engineering, Seoul National University, Seoul 08826, Republic of Korea;

orcid.org/0000-0002-6449-6725; Email: twlees@snu.ac.kr, taewlees@gmail.com

Authors

Sung-Joo Kwon – Department of Materials Science and Engineering, Pohang University of Science and Technology (POSTECH), Pohang, Gyungbuk 790-784, Republic of Korea

Soyeong Ahn – Department of Materials Science and Engineering, Pohang University of Science and Technology (POSTECH), Pohang, Gyungbuk 790-784, Republic of Korea

Jung-Min Heo – Department of Materials Science and Engineering, Seoul National University, Seoul 08826, Republic of Korea

Dong Jin Kim – Program in Nano Science and Technology, Graduate School of Convergence Science and Technology, Seoul National University, Seoul 08826, Republic of Korea

Jinwoo Park – Department of Materials Science and Engineering, Seoul National University, Seoul 08826, Republic of Korea

Hae-Ryung Lee – Department of Materials Science and Engineering and Research Institute of Advanced Materials, Seoul National University, Seoul 08826, Republic of Korea

Sungjin Kim – Department of Materials Science and Engineering, Seoul National University, Seoul 08826, Republic of Korea

Huanyu Zhou – Department of Materials Science and Engineering, Seoul National University, Seoul 08826, Republic of Korea

Min-Ho Park – Department of Materials Science and Engineering and Research Institute of Advanced Materials, Seoul National University, Seoul 08826, Republic of Korea

Young-Hoon Kim – Research Institute of Advanced Materials, Seoul National University, Seoul 08826, Republic of Korea

Wanhee Lee – Department of Materials Science and Engineering, Seoul National University, Seoul 08826, Republic of Korea

Jeong-Yun Sun – Department of Materials Science and Engineering and Research Institute of Advanced Materials, Seoul National University, Seoul 08826, Republic of Korea;

orcid.org/0000-0002-7276-1947

Byung Hee Hong – Department of Chemistry, Seoul National University, Seoul 08826, Republic of Korea; Graphene Research Center Advanced Institute of Convergence Technology, Suwon 16229, Republic of Korea; orcid.org/0000-0001-8355-8875

Complete contact information is available at:
<https://pubs.acs.org/10.1021/acsami.0c12939>

Author Contributions

[†]S.-J.K., S.A., and J.-M.H. contributed equally to this work.

Notes

The authors declare no competing financial interest.

ACKNOWLEDGMENTS

This work was supported by the National Research Foundation of Korea (NRF) grant funded by the Korea government (Ministry of Science, ICT & Future Planning) (NRF-2016R1A3B1908431). Also, this work was supported by the 10079974 Development of Core Technologies on Materials, Devices, and Processes for TFT backplane and light emitting frontplane with enhanced stretchability above 20%, with application to stretchable display.

REFERENCES

- (1) Kim, Y.-H.; Cho, H.; Lee, T.-W. Metal Halide Perovskite Light Emitters. *Proc. Natl. Acad. Sci. U.S.A.* **2016**, *113*, 11694–11702.
- (2) Cho, H.; Jeong, S.-H.; Park, M.-H.; Kim, Y.-H.; Wolf, C.; Lee, C.-L.; Heo, J. H.; Sadhanala, A.; Myoung, N.; Yoo, S.; Im, S. H.; Friend, R. H.; Lee, T.-W. Overcoming the Electroluminescence Efficiency Limitations of Perovskite Light-Emitting Diodes. *Science* **2015**, *350*, 1222–1225.
- (3) Kim, Y.-H.; Wolf, C.; Kim, Y.-T.; Cho, H.; Kwon, W.; Do, S.; Sadhanala, A.; Park, C. G.; Rhee, S.-W.; Im, S. H.; Friend, R. H.; Lee, T.-W. Highly Efficient Light-Emitting Diodes of Colloidal Metal–Halide Perovskite Nanocrystals beyond Quantum Size. *ACS Nano* **2017**, *11*, 6586–6593.
- (4) Kim, Y.-H.; Cho, H.; Heo, J. H.; Kim, T.-S.; Myoung, N.; Lee, C.-L.; Im, S. H.; Lee, T.-W. Multicolored Organic/Inorganic Hybrid Perovskite Light-Emitting Diodes. *Adv. Mater.* **2015**, *27*, 1248–1254.
- (5) Seo, H.-K.; Kim, H.; Lee, J.; Park, M.-H.; Jeong, S.-H.; Kim, Y.-H.; Kwon, S.-J.; Han, T.-H.; Yoo, S.; Lee, T.-W. Efficient Flexible Organic/Inorganic Hybrid Perovskite Light-Emitting Diodes Based on Graphene Anode. *Adv. Mater.* **2017**, *29*, 1605587.
- (6) Ahn, S.; Park, M. H.; Jeong, S. H.; Kim, Y. H.; Park, J.; Kim, S.; Kim, H.; Cho, H.; Wolf, C.; Pei, M.; Yang, H.; Lee, T. W. Fine Control of Perovskite Crystallization and Reducing Luminescence Quenching

Using Self-Doped Polyaniline Hole Injection Layer for Efficient Perovskite Light-Emitting Diodes. *Adv. Funct. Mater.* **2019**, *29*, 1807535.

(7) Jeong, S.-H.; Woo, S.-H.; Han, T.-H.; Park, M.-H.; Cho, H.; Kim, Y.-H.; Cho, H.; Kim, H.; Yoo, S.; Lee, T.-W. Universal High Work Function Flexible Anode for Simplified ITO-Free Organic and Perovskite Light-Emitting Diodes with Ultra-High Efficiency. *NPG Asia Mater.* **2017**, *9*, No. e411.

(8) Nair, R. R.; Wu, H. A.; Jayaram, P. N.; Grigorieva, I. V.; Geim, A. K. Unimpeded Permeation of Water Through Helium-Leak-Tight Graphene-Based Membranes. *Science* **2012**, *335*, 442–444.

(9) Han, T.-H.; Kim, H.; Kwon, S.-J.; Lee, T.-W. Graphene-Based Flexible Electronic Devices. *Mater. Sci. Eng., R* **2017**, *118*, 1–43.

(10) Koenig, S. P.; Wang, L.; Pellegrino, J.; Bunch, J. S. Selective Molecular Sieving Through Porous Graphene. *Nat. Nanotechnol.* **2012**, *7*, 728–732.

(11) Surwade, S. P.; Smirnov, S. N.; Vlassiok, I. V.; Unocic, R. R.; Veith, G. M.; Dai, S.; Mahurin, S. M. Water Desalination using Nanoporous Single-Layer Graphene. *Nat. Nanotechnol.* **2015**, *10*, 459–464.

(12) Seo, H.-K.; Park, M.-H.; Kim, Y.-H.; Kwon, S.-J.; Jeong, S.-H.; Lee, T.-W. Laminated Graphene Films for Flexible Transparent Thin Film Encapsulation. *ACS Appl. Mater. Interfaces* **2016**, *8*, 14725–14731.

(13) Yamaguchi, H.; Granstrom, J.; Nie, W.; Sojoudi, H.; Fujita, T.; Voiry, D.; Chen, M.; Gupta, G.; Mohite, A. D.; Graham, S.; Chhowalla, M. Reduced Graphene Oxide Thin Films as Ultrabarrriers for Organic Electronics. *Adv. Energy Mater.* **2014**, *4*, 1300986.

(14) Choi, K.; Nam, S.; Lee, Y.; Lee, M.; Jang, J.; Kim, S. J.; Jeong, Y. J.; Kim, H.; Bae, S.; Yoo, J.-B.; Cho, S. M.; Choi, J.-B.; Chung, H. K.; Ahn, J.-H.; Park, C. E.; Hong, B. H. Reduced Water Vapor Transmission Rate of Graphene Gas Barrier Films for Flexible Organic Field-Effect Transistors. *ACS Nano* **2015**, *9*, 5818.

(15) Li, X.; Cai, W.; An, J.; Kim, S.; Nah, J.; Yang, D.; Piner, R.; Velamakanni, A.; Jung, I.; Tutuc, E.; Banerjee, S. K.; Colombo, L.; Ruoff, R. S. Large-Area Synthesis of High-Quality and Uniform Graphene Films on Copper Foils. *Science* **2009**, *324*, 1312.

(16) Liu, N.; Chortos, A.; Lei, T.; Jin, L.; Kim, T. R.; Bao, W.-G.; Zhu, C.; Wang, S.; Pfattner, R.; Chen, X.; Sinclair, R.; Bao, Z. Ultra-transparent and Stretchable Graphene Electrodes. *Sci. Adv.* **2017**, *3*, No. e1700159.

(17) Yambem, S. D.; Liao, K.-S.; Alley, N. J.; Curran, S. A. Stable Organic Photovoltaics using Ag Thin Film Anodes. *J. Mater. Chem.* **2012**, *22*, 6894–6898.

(18) Lee, D.; Lee, H.; Ahn, Y.; Jeong, Y.; Lee, D.-Y.; Lee, Y. Highly Stable and Flexible Silver Nanowire–Graphene Hybrid Transparent Conducting Electrodes for Emerging Optoelectronic Devices. *Nanoscale* **2013**, *5*, 7750.

(19) Han, T.-H.; Kwon, S.-J.; Seo, H.-K.; Lee, T.-W. Controlled Surface Oxidation of Multi-Layered Graphene Anode to Increase Hole Injection Efficiency in Organic Electronic Devices. *2D Mater.* **2016**, *3*, 014003.

(20) Kim, Y.-H.; Lee, G.-H.; Kim, Y.-T.; Wolf, C.; Yun, H. J.; Kwon, W.; Park, C. G.; Lee, T.-W. High Efficiency Perovskite Light-Emitting Diodes of Ligand-Engineered Colloidal Formamidinium Lead Bromide Nanoparticles. *Nano Energy* **2017**, *38*, 51.

(21) Kwon, S.-J.; Han, T.-H.; Ko, T. Y.; Li, N.; Kim, Y.; Kim, D. J.; Bae, S.-H.; Yang, Y.; Hong, B. H.; Kim, K. S.; Ryu, S.; Lee, T.-W. Extremely Stable Graphene Electrodes Doped with Macromolecular Acid. *Nat. Commun.* **2018**, *9*, 2037.

(22) Han, T.-H.; Kwon, S.-J.; Li, N.; Seo, H.-K.; Xu, W.; Kim, K. S.; Lee, T.-W. Versatile p-Type Chemical Doping to Achieve Ideal Flexible Graphene Electrodes. *Angew. Chem., Int. Ed.* **2016**, *55*, 6197.

(23) Choi, M.-R.; Han, T.-H.; Lim, K.-G.; Woo, S.-H.; Huh, D. H.; Lee, T.-W. Soluble Self-Doped Conducting Polymer Compositions with Tunable Work Function as Hole Injection/Extraction Layers in Organic Optoelectronics. *Angew. Chem., Int. Ed.* **2016**, *55*, 6197.